Parameter Optimization for FEM based modeling of singlet oxygen during PDT using COMSOL

Xing Liang[1], Ken Kang-Hsin Wang[1], and Timothy C. Zhu[1*]
[1]Department of Radiation Oncology, School of Medicine, University of Pennsylvania, Philadelphia, PA 19104
*Corresponding author: Radiation Oncology, University of Pennsylvania, 3400 Spruce Street/2 Donner Bldg, Philadelphia, PA 19104, tzhu@mail.med.upenn.edu

Abstract: Singlet oxygen ($^1O_2$) is the major cytotoxic agent in photodynamic therapy (PDT). The reaction between $^1O_2$ and tumor cells defines the treatment efficacy. Based on a previously developed model that incorporates the diffusion equation for the light transport in tissue and the macroscopic kinetic equations for the generation of the singlet oxygen, the distance-dependent reacted $^1O_2$ was numerically calculated using finite-element method (FEM) on COMSOL. The formula of reacted $^1O_2$ concentration involves 5 photo-physiological parameters which need to be determined explicitly to predict the generation of $^1O_2$. We developed an algorithm to iteratively calculate the singlet oxygen concentration profile and compared with the measurements to obtain an optimal set of parameters. The optimization is performed using Matlab and dynamically linked with the COMSOL for the forward calculation. The optimized parameters were then used to predict the transient apparent reacted $^1O_2$ concentration as a PDT dosimetry quantity on a 3D prostate model in COMSOL.

Keywords: Singlet oxygen, PDT dosimetry, macroscopic model, microscopic model, oxygen consumption, dynamic mechanism.

1. Introduction

Photodynamic therapy (PDT) is an important treatment modality for cancer and other localized diseases. During the treatment, photosensitizers excited by light react with ground state oxygen $^3O_2$, which leads to generation of the major cyto-toxic agent - singlet oxygen $^1O_2$ - to kill the surrounding tissues and cells. Compared with other treatments, PDT has its unique advantages. First, light can be delivered only to region of interest, to increase specificity. Second, PDT is a non-ionizing modality thus avoiding potential cumulative radiation effects. Finally, PDT usually combines faster post operative recovery and better cosmetic outcome. However, one major deficiency of current PDT technology is the lack of accurate dosimetry to assess PDT efficacy. We have been focusing on developing an explicit PDT dosimetry model using apparent reacted $^1O_2$ concentration, $[^1O_2]_{rx}$, as the clinical PDT dosimetry quantity [1-3]. Finite element method (FEM) was used to model the complex geometry in human anatomy.

In this paper, a new optimization algorithm was implemented based on the previous model, in which PDT spatial-dependent light distribution was modeled in COMSOL, and time-dependent $[^1O_2]_{rx}$ was modeled in Matlab dynamically linked with COMSOL. Once the spatial light distribution was determined, the optimization algorithm compared the model with experimental necrosis radius from mice studies, and determined the optimal photophysiological parameters. PDT dosimetry prediction using $[^1O_2]_{rx}$ was then obtained using these parameters, and based on prostate ultrasound images. The flow chart of this work is shown Fig. 1, in which the red arrows represent processes implemented by COMSOL, while blue arrows represent processes implemented by MATLAB dynamically linked with COMSOL.

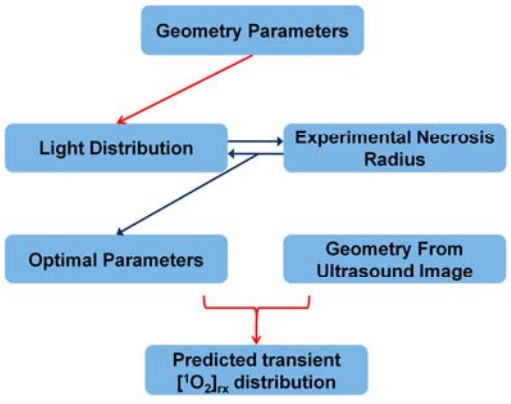

Figure 1. Flow chart for PDT photophysiological parameter optimization and dosimetry prediction. Red arrows denote COMSOL process, while blue arrows denote Matlab + COMSOL process.

2. Method

The governing equations describe the dynamic process that determines the absorption of light, ϕ, the consumption of photosensitizing drug, [S], oxygen [$^3O_2$], and the production of singlet oxygen, [$^1O_2$]. For simplicity, all the calculations were carried out either in one-dimension for a spherical geometry or in two-dimension for a semi-infinite geometry.

2.1 Singlet oxygen model

The following are the governing equations of our macroscopic singlet oxygen model.

$$(\mu_a + \varepsilon \cdot u_2)u_1 - \nabla \cdot \left(\frac{1}{3\mu_s'}\nabla u_1\right) = S \quad (1)$$

$$\frac{du_2}{dt} + \left(S_\Delta \gamma\eta \frac{\kappa}{1+\alpha}\frac{u_1(u_2+\delta)u_3}{u_3+\beta}\right)u_2 = 0 \quad (2)$$

$$\frac{du_3}{dt} + \left(S_\Delta \gamma\eta \frac{\alpha}{1+\alpha}\frac{u_1u_2}{u_3+\beta}\right)u_3 - g\left(1-\frac{u_3}{u_3(t=0)}\right) = 0 \quad (3)$$

$$\frac{du_4}{dt} - \left(fS_\Delta \gamma\eta \frac{\alpha}{1+\alpha}\frac{u_1u_2u_3}{u_3+\beta}\right) = 0 \quad (4)$$

where u_1, u_2, u_3, and u_4 represent light fluence rate ϕ, the concentrations of sensitizer [S_0], oxygen [$^3O_2$], and reacted singlet oxygen [$^1O_2$], respectively. In the cases we considered here μ_a, μ_s', ε, and S are the absorption, reduced scattering coefficients at treatment wavelength, extinction coefficient for photosensitizer at the treatment wavelength, and source strength in mW/cm for a linear source, respectively. α, β, γ, κ, η and S_Δ are the photophysical parameters for photosensitizer. The detail of the origin and definition can be found in [3]. g is the maximum oxygen supply rate, and f is the fraction of $[^1O_2]_{rx}$ efficiently inducing cell death. In this work, we assume f equal to one. $[^1O_2]_{rx}$ is the $[^1O_2]$ reacting with cell targets, which is the dosimetry quantity fundamentally determining the treatment efficacy, and can be described as

$$[^1O_2]_{rx} = \int_0^T [^1O_2]dt \quad (5)$$

Compared with the model used in our previous works [2-4], a new parameter δ is introduced in the current model, which is a low photosensitizer concentration correction term [5-8]. In most clinical environments, the sensitizer concentration is low enough that the $^1O_2$ molecule is more likely to react with its parent sensitizer than would be predicted based solely on the species' relative concentrations. Therefore, the introduction of the δ term improves the theoretical description of the bleaching mechanism in a low photosensitizer concentration environment.

In the optimization process, Eq. (1) is considered as a steady state equation, and being solved independently from the other three time dependent Eqs. (2-4). The complex photochemical parameters can be further lumped into 3 independent parameters, where $\xi = S_\Delta\gamma\eta\alpha/(1+\alpha)$, $\sigma = \kappa/\alpha$, and β. The final modeling equations can be described as

$$\mu_a u_1 - \nabla \cdot \left(\frac{1}{3\mu_s'}\nabla u_1\right) = S \quad (6)$$

$$\frac{du_2}{dt} + \left(\xi\sigma \frac{u_1(u_2+\delta)u_3}{u_3+\beta}\right)u_2 = 0 \quad (7)$$

$$\frac{du_3}{dt} + \left(\xi \frac{u_1u_2}{u_3+\beta}\right)u_3 - g\left(1-\frac{u_3}{u_3(t=0)}\right) = 0 \quad (8)$$

$$\frac{du_4}{dt} - \left(\xi \frac{u_1u_2u_3}{u_3+\beta}\right) = 0 \quad (9)$$

In Eq. 6, $\varepsilon \cdot u_2$ is dropped, because in the study, the sensitizer extinction coefficient ε is set to be 0.0035 (cm^{-1} uM^{-1}) [9] and the initial *in vivo* Photofrin concentration is assumed to be 7 μM, 24 hr after 5 mg/kg *i.v.* injection [4]. The absorption coefficient for Photofrin is 0.025 cm^{-1} which is 28 folder lower than the absorption coefficient of tumor tissue such as 0.71 (cm^{-1}) measured interstitially (data not shown). Therefore, the 4 independent parameters g, ξ, σ, and β needs to be determined precisely using the optimization algorithm.

2.2 Parameter optimization

In the optimization process, the main program was coded in MATLAB environment which executes calculation procedure by calling COMSOL model. First, the steady state light diffusion equation (Eq. (6)) for a linear source in a 3D cylindrical geometry was built in a COMSOL environment. Due to the symmetrical feature of the cylinder, we are only interested in the light distribution along 1D radial axis. This 1D light distribution profile will be passed to

next step, the calculation of PDT kinetics equation (Eqs. (7-9)). Again, due to the cylindrically-symmetrical feature, we can consider the $[^1O_2]_{rx}$ production in 1D radial axis. A fitting quantity $[^1O_2]_{rx,sd}$ was introduced in the algorithm to represent "apparent singlet oxygen threshold concentration". During the process, our fitting routine varies the 4 independent parameters globally so that the $[^1O_2]_{rx}$ at the necrotic radius for each animal is close to the $[^1O_2]_{rx,sd}$. In the current fitting routine, an initial guess of $[^1O_2]_{rx,sd}$ is assigned randomly within the range of 0.4 to 1.1 mM and the value is fixed throughout the subsequent fitting procedure. The differential evolution algorithm developed by Storn *et al.* [10] and modified by us are used as the optimization routine. It is an efficient direct-search algorithm for nonlinear problem. Our goal is to minimize the maximum deviation MAX ($|[^1O_2]_{rx}/[^1O_2]_{rx,sd} - 1|$) between data and fit. The algorithm was implemented in MATLAB using function fminsearch, and a certain number of iterations were calculated to give the optimized parameters. The necrosis distances from different treatment conditions were obtained from 12 *in vivo* mice experiments. Table 1 lists the boundary, initial conditions, and other necessary parameters used in this model [2].

Table 1. Boundary, initial conditions, and parameters for singlet oxygen model

Boundary conditions	$u_{i=2,3,4}$	$\nabla u_i = 0$
Initial conditions	u_2 (μM)	7
	u_3 (μM)	83
	u_4 (μM)	0
Light associated parameters	μ_a (cm^{-1})	0.71
	μ_s' (cm^{-1})	9.14
Physiological parameter	δ (μM)	33
	g (mM)	0.7
Photochemical Parameter (for Photofrin)	ξ (cm^2/mWs)	3.7×10^{-3}
	σ (1/μM)	7.6×10^{-5}
	β (μM)	11.9

The values of the initial conditions of u_2 and u_3 are extracted from *in vivo* experiment. The values of μ_a and μ_s' are determined by interstitial point source technique [11] within RIF mice tumor. The result of this optimization fitting is a single set of the parameters g, ξ, σ, and β.

2.3 Reacted singlet oxygen concentration prediction

Once the optimal photophysiological parameters were determined, they were used to calculate the $[^1O_2]_{rx}$ for any geometry as a PDT dosimetry quantity. COMSOL Multiphysics was used to model the PDT reacted singlet oxygen concentration. The light distribution (Eq. 6) was modeled using PDE mode in COMSOL, while PDT kinetics equation (Eqs. (7-9)) were modeled using time-dependent PDE mode. The geometry and optical properties of the PDT dosimetry utilized the human prostate reconstruction previously introduced [12]. Briefly, in COMSOL meshes were generated in the 3D prostate geometry, reconstructed using transrectal ultrasound images of a treated prostate. Optical properties were assumed to be homogeneous in the prostate in the calculation, including μ_a = 0.3 cm^{-1} and μ_s' = 14 cm^{-1}. The refractive indices were assumed to be 1.4 and 1.0 for the prostate and the cylindrical surrounding layer, respectively. 12 linear sources were modeled for treatment, and intensity of 150 mW/cm^2 was used for each source. A 3-D geometry of the patient's prostate was reconstructed and shown in Fig. 2, as well as the mesh plot of the geometry. Photosensitizer used in the prediction model is Photofrin.

3. Results and Discussions

3.1 Numerical results simulating *in vivo* Photofrin-PDT treatment

From the optimization process described in 2.2, an optimized set of parameters g, ξ, σ, and β are obtained, as shown in table 2. These photochemical parameters are also compared with our previous fitting results and reported values for PDT application of Photofrin at 630 nm from literatures. It is obvious that the photochemical oxygen consumption rate per light fluence rate ξ has a lower value compared with previous results. The probability ratio of a $^1O_2$ molecule reacting with ground-state

photosensitizer compared to the $^1O_2$ molecule reacting with a cellular target σ has a much larger value. The ratio of the monomolecular decay rate of the triplet state photosensitizer to the bimolecular rate of the triplet photosensitizer quenching by $^3O_2$ β remain the same, while maximum oxygen supply rate g and apparent singlet oxygen threshold concentration $[^1O_2]_{rx,sd}$ were calculated as 0.8 mM/s and 0.41mM/s, respectively. At the optimal parameters, the result of fitting the PDT-induced necrotic radius with the calculated photo sensitizer concentration, triplet oxygen concentration and apparent reacted singlet oxygen concentration are shown in Fig. 3. The symbols represent the necrotic radius for 12 different mice. One can notice in Fig. 3 that the apparent reacted singlet oxygen concentration decrease with the radius increase, mainly due to the light distribution decrease over distance in tissue.

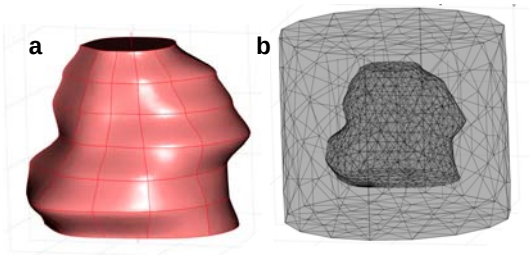

Figure 2. Reconstructed prostate geometry. (a) Prostate Geometry surface. (b) Mesh plot of the prostate with a surrounding cylindrical layer.

Table 2. Parameters from optimization process

Parameters	Final fit	Previous fit [1]	Published values
ξ ($cm^2/s/mW$)	**2.0×10^{-3}**	2.1×10^{-3}	3.7×10^{-3} [6]
σ (1/mM)	**11.2×10^{-5}**	7.6×10^{-3}	7.6×10^{-3} [6]
β (mM)	**11.9**	11.9	11.9 [13]
g (mM/s)	**0.8**	0.69	–
$[^1O_2]_{rx,sh}$ (mM)	**0.41**	0.74	–

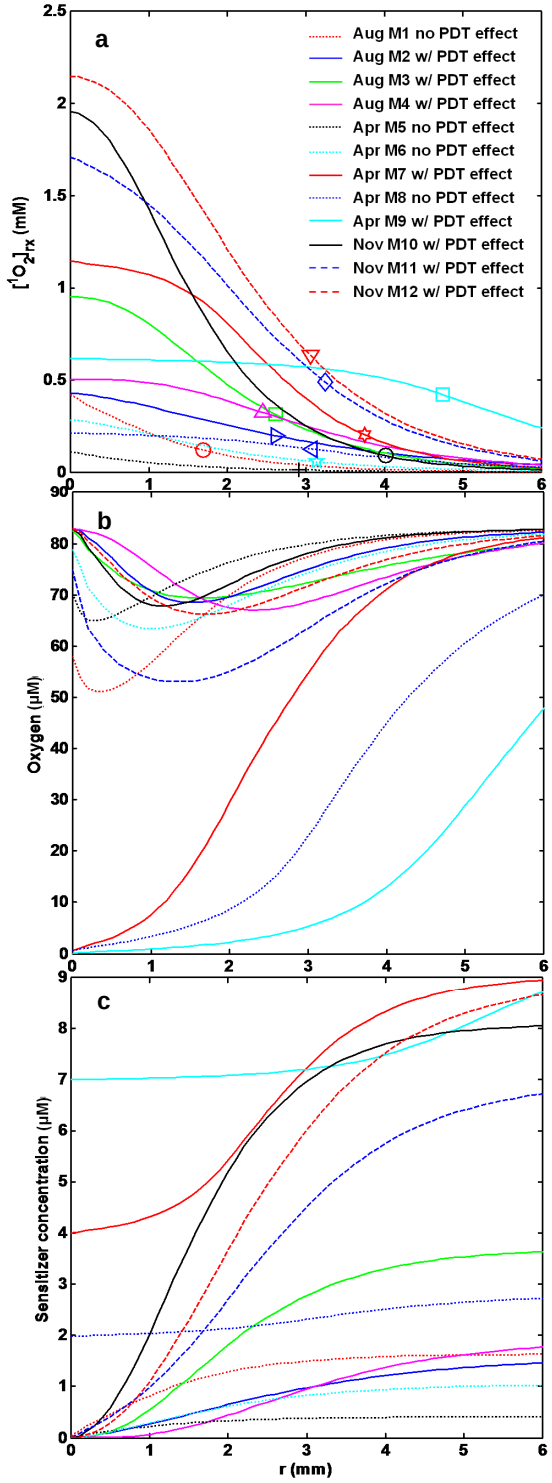

Figure 3: Results for optimization calculation. (a) Sensitizer, (b) oxygen, and (c) reacted singlet oxygen concentrations as functions of necrosis radius from 12 mice.

3.2 Results of PDT treatment simulation using optimal parameters

Using the calculated parameters in Table 2, we are able to predict PDT quantities in a rather complex geometry, which was described in 2.3. The prediction resutls are shown in Fig. 4. Fig. 4a demonstrates apparent reacted singlet oxygen concentration distribution in the prostate and surrounding cylinder model at 300 s of treatment. Slices in x-y and y-z planes are used to better visualize the results. The same result is also shown in Fig. 4b, in which the isosurface of 0.41 mM (apparent singlet oxygen threshold concentration) was plotted for the purpose of visualizing treatment efficacy. Fig. 4c shows the light fluence rate distribution at 300 s of treatment.

It is obvious that from our prediction model, the apparent reacted singlet oxygen above threshold is not covering the whole prostate at 300 s, which means the treatment is not completed at this time point. However, if one uses light fluence distribution in treatment prediction (as in [12]), it is not clear how well the treatment has been applied. To better understand the prediction model, top views of apparent reacted singlet oxygen concentration distribution and light fluence distribution are shown in Fig. 5, in which Fig. 5a and d are results at treatment time of 200 s, Fig. 5b and e are results at treatment time of 500 s, while Fig. 5c and f are results at treatment time of 1000 s. The apparent reacted singlet oxygen concentration distribution starts from close to the linear sources, and almost cover the whole prostate model at 500 s, but still with some gaps for treatment. At 1000 s of treatment, the whole prostate is treated completely. From this model, the time threshold for a complete PDT treatment on the prostate model is ~560 s. This prediction model precisely estimate the clinical PDT dosimetry quantity $[^1O_2]_{rx}$, which may help assess PDT treatment efficacy accurately. On the other hand, it may be difficult to predict PDT dosimetry from light fluence distribution, as it can hardly predict the treatment efficacy over time.

4. Conclusions

Finite element method from COMSOL was applied to model light fluence rate distribution in PDT, combined with optimization algorithm implemented in MATLB to calculate the macroscopic kinetic equations for the generation of the singlet oxygen and photochemical parameters. Four photochemical parameters g, ξ, σ, and β were obtained from the optimization process. Using the optimal parameters, apparent singlet oxygen concentration can be calculated and used as an improved dosimetry quantity. Compared with previous PDT dose (light distribution), $[^1O_2]_{rx}$ is a dosimetry quantity with

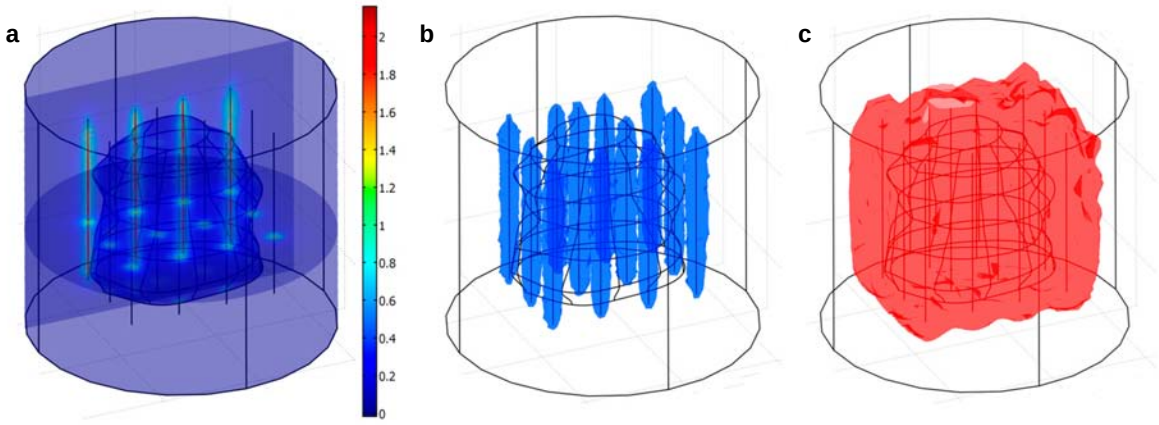

Figure 4: Results of PDT dosimetry quantities for treatment up to 300 s in a homogeneous prostate with μ_a = 0.3 cm^{-1} and μ_s' = 14 cm^{-1} and uniform source strength loading assumption. (a) Slides demonstration of apparent reacted singlet oxygen concentration distribution. Unit for color bar is mM. (b) Isosurface demonstration of apparent reacted singlet oxygen concentration distribution for treatment up to $[^1O_2]_{rx,sd}$ = 0.41 mM. (c) Isosurface demonstration of light fluence rate distribution at 100 mW/cm^2.

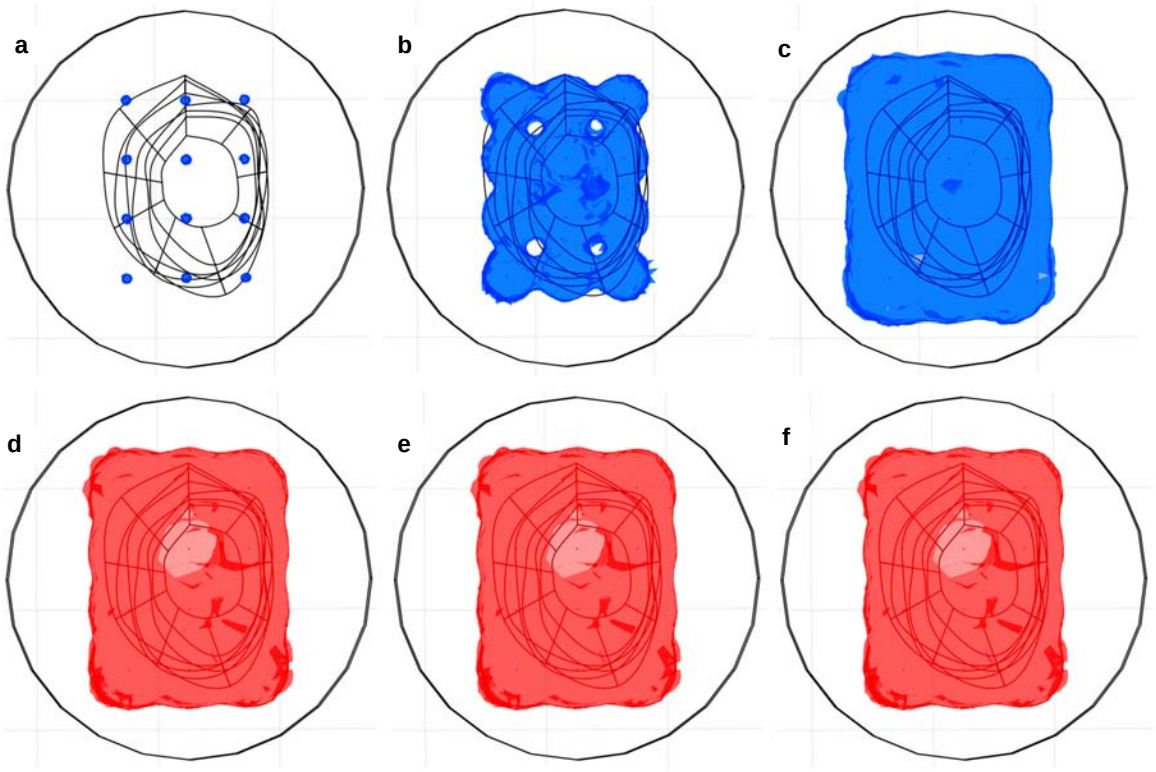

Figure 5: Isosurface results of PDT dose quantities at different treatment time. (a) $[^1O_2]_{rx}$ at 0.41 mM at 200 s. (b) $[^1O_2]_{rx}$ at 0.41 mM at 500 s. (c) $[^1O_2]_{rx}$ at 0.41 mM at 1000 s. (d) Light fluence distribution for 30 J/cm^2 at 200 s. (e) Light fluence distribution for 75 J/cm^2 at 500 s. (f) Light fluence rate distribution at 150 J/cm^2 at 1000 s.

better accuracy, especially in the way to demonstrate time-dependant PDT treatment efficacy. These optimal parameters were also applied to a 3D prostate geometry, to compare the PDT dosimetry quantities in time-dependent simulation implemented in COMSOL.

5. Acknowledgements

This work is supported by grants from National Institute of Health (NIH) R01 CA 109456 and P01 CA 87971.

6. References

1. S. B. Brown, E. A. Brown, and I. Walker, "The present and future role of photodynamic therapy in cancer treatment," Lancet Oncol. **5**, 497-508 (2004).
2. K.-H. K. Wang, M. T. Busch, J. C. Finlay, and T. C. Zhu, "Optimization of physiological parameter for macroscopic modeling of reacted singlet oxygen concentration in an *in-vivo* model," Proc. of SPIE **7164**, 71640O (2009).
3. T. C. Zhu and X. Zhou, "Finite-element modeling of singlet oxygen during photodynamic therapy," Proc. COMSOL Multiphysics, 189-195 (2007).
4. T. C. Zhu, J. C. Finlay, X. Zhou, and J. Li, "Macroscopic modeling of the singlet oxygen

prodution during PDT," Proc. SPIE **6427**, 642708 642701-642712 (2007).

5. K. K. Wang, J. C. Finlay, T. M. Busch, S. M. Hahn, and T. C, Zhu, "Explicit dosimetry for photodynamic therapy: macroscopic singlet oxygen modeling," J. Biophoton. **3**, 1-15, 2010.
6. K. K. Wang, S. Mitra, and T. H. Foster, "A comprehensive mathematical model of microscopic dose deposition in photodynamic therapy," Med. Phys. **34**, 282–293 (2007).
7. J. S. Dysart, G. Singh, and M. S. Patterson, "Calculation of singlet oxygen dose from photosensitizer fluorescence and photobleaching during mTHPC Photodynamic Therapy of MLL Cells," Photochem. Photobiol. **81**, 196–205 (2005).
8. K. K. Wang, and T. C. Zhu, " Explicit dosimetry for photodynamic therapy; singlet xxygen modeling based on finite-element method" Proc. COMSOL Multiphysics, (2009).
9. S. Mitra, and T. H. Foster, "Photophysical parameters, photosensitizer retention and tissue optical properties completely account for the higher photodynamic efficacy of meso-tetra-hydroxyphenyl-chlorin vs Photofrin," Photochem. Photobiol. **81**, 849-859 (2005).
10. R. Storn and K. Price, "Differential evolution-A simple and efficient heuristic for global optimization over continuous spaces," J. Global Optimization **11**, 341-359 (1996).
11. A. Dimofte, J. C. Finlay, and T. C. Zhu, "A method for determination of the absorption and scattering properties interstitially in turbid media," Phys. Med. Biol. **50**, 2291-2311 (2005).
12. J. Li, T. C. Zhu, and J. C. Finlay, "Study of light fluence rate distribution in photodynamic therapy using finite-element method," Proc. SPIE **6139**, 61390M-1 - 61390M-8 (2006).
13. I. Georgakoudi , M. G. Nichols, and T. H. Foster, "The mechanism of photofrin photobleaching and its consequences for photodynamic dosimetry," Photochem. Photobiol. **65**, 135–144 (1997).